NANO LETTERS

LETTER

pubs.acs.org/NanoLett

Optical Forces in Hybrid Plasmonic Waveguides

Xiaodong Yang,[†,‡] Yongmin Liu,[‡] Rupert F. Oulton,[‡] Xiaobo Yin,[†,‡] and Xiang Zhang*[,†,‡]

[†]Materials Sciences Division, Lawrence Berkeley National Laboratory, 1 Cyclotron Road, Berkeley, California 94720, United States

[‡]NSF Nanoscale Science and Engineering Center, 3112 Etcheverry Hall, University of California, Berkeley, California 94720, United States

ABSTRACT: We demonstrate that in a hybrid plasmonic system the optical force exerted on a dielectric waveguide by a metallic substrate is enhanced by more than 1 order of magnitude compared to the force between a photonic waveguide and a dielectric substrate. A nanoscale gap between the dielectric waveguide and the metallic substrate leads to deep subwavelength optical energy confinement with ultralow mode propagation loss and hence results in the enhanced optical forces at low input optical power, as numerically demonstrated by both Maxwell's stress tensor formalism and the coupled mode theory analysis. Moreover, the hybridization between the surface plasmon modes and waveguide modes allows efficient optical trapping of single dielectric nanoparticle with size of only several nanometers in the gap region, manifesting various optomechanical applications such as nanoscale optical tweezers.

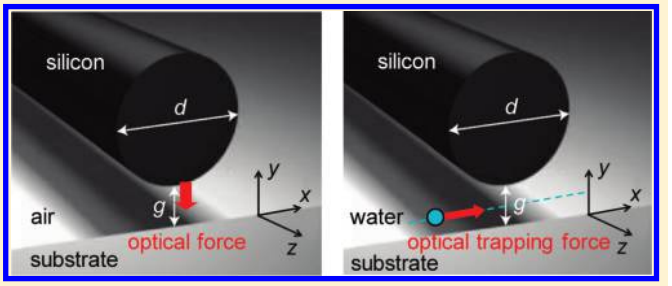

KEYWORDS: Optical force, optical trapping, surface plasmon polariton, hybrid plasmonic waveguide

Optical force generated from the gradient of the light field has been widely used in optical tweezers.[1,2] It has been recently demonstrated that the transverse gradient optical force can be increased by orders of magnitude in coupled optical waveguides due to the largely enhanced gradient of the optical field.[3−5] The forces can be boosted furthermore with coupled high-*Q* optical resonators[6−9] where the circulating optical power is significantly amplified due to the long photon lifetime. Such gradient optical forces have been broadly exploited in dielectric nanostructures to realize many exciting applications for light-matter interactions, for example, optical amplification and cooling of mechanical modes,[10] actuation of nanophotonic structures,[4,5,8,9] optomechanical wavelength and energy conversion,[11] all-optical signal processing,[12] sensitive mechanical sensors,[13] and optical trapping and transport of nanoparticles and biomolecules.[14,15]

Surface plasmon polaritons (SPPs), the collective optical excitations of electrons along a metal-dielectric interface,[16,17] bring new capabilities in confining electromagnetic waves to deep subwavelength scale.[18,19] Such a strong optical confinement results in significantly enhanced optical field strength and gradient of light field, which will greatly enhance the optical force. Recently, gradient optical forces have been investigated in various plasmonic nanostructures, for example, gold nanoparticle dimers[20] and coupled metal planar waveguides.[21] On the basis of plasmonic nanostructures with subwavelength mode volume, nanoscale optical tweezers with trapping volume beyond the diffraction limit can also be realized for optical trapping of a single nanoparticle.[22−25] However, the resulting gradient optical forces at certain input optical power are still limited by the ohmic loss of the plasmonic modes, where a huge amount of optical energy will be dissipated into the heat that will not contribute to the mechanical work.

On the other hand, the hybrid plasmonic waveguide has much lower propagation loss while maintaining deep-subwavelength optical mode confinement, resulting in applications utilizing the strong light-matter interactions such as plasmonic nanolasers.[26,27] In this paper, we demonstrate that the gradient optical force exerted on a hybrid plasmonic waveguide can be enhanced over ten times, compared to the optical force generated in a conventional photonic waveguide with a dielectric substrate underneath.[4] This enhancement arises from the deep subwavelength optical energy confinement of the hybrid plasmonic mode and the relatively low loss. The structural dependence of the optical forces and the optimized waveguide design are systematically analyzed with both Maxwell's stress tensor formalism and the coupled mode theory to reveal the mechanism of this enhanced optical force. We also demonstrate that the optical trapping force applied on a single dielectric nanoparticle can be strongly enhanced utilizing the hybrid plasmonic mode. Such an interesting result may be useful to design nanoscale optical tweezers to manipulate a single nanoscale object such as a biomolecule or one quantum dot.

Figure 1a shows the geometry of the coupled waveguide system of our interest. A high-refractive-index dielectric cylinder waveguide with diameter d is coupled to a metallic substrate or a dielectric substrate with nanoscale air gap g in between, which forms a hybrid plasmonic waveguide or a photonic waveguide, respectively. The cylinder waveguide is silicon with the refractive index $n = 3.5$, and the metallic substrate is silver with a permittivity of $(-129 + 3.3i)$ at telecommunication wavelength

Received: August 30, 2010
Revised: November 4, 2010
Published: January 13, 2011

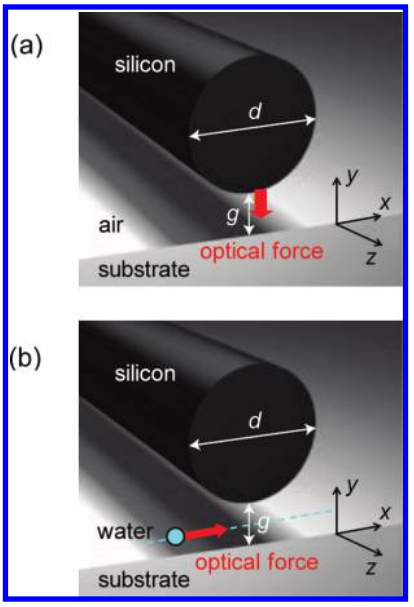

Figure 1. (a) The geometry of the coupled waveguide system with a dielectric cylinder waveguide above the substrate with a nanoscale gap in between. An attractive optical force will be exerted on the waveguide due to the coupling between the waveguide mode and the substrate mode. (b) The optical trapping force will be applied on a single nanoparticle toward the center of the nanoscale gap.

1550 nm.[28] The strong coupling between the dielectric waveguide cylinder mode and the SPP mode supported at the interface of air and silver results in an extremely confined hybrid plasmonic mode, while the evanescent coupling between the cylinder mode and the glass substrate acts as a perturbation to the photonic mode as elaborated below. The finite-element analysis method (COMSOL) is used to calculate the eigenmode of the coupled waveguide system.

Figure 2a shows the dispersion relation of the hybrid plasmonic mode with waveguide diameter d = 250 nm for different air gaps. As expected, guided hybrid plasmonic modes locate beyond the light cone. At fixed wavevector $\mathbf{k}$, the frequency of the eigenmode decreases as the gap g is reduced. To better understand the optical force enhancement, we first study the mode properties of the hybrid plasmonic mode. Figure 2b,c shows the mode area A_m and the propagation length L_m of the hybrid plasmonic mode depended on the waveguide diameter d and the air gap g. The mode area is calculated from $A_m = W_m/\max[W(r)]$, where W_m and $W(r)$ are the integrated electromagnetic energy over the entire space and the local energy density at the position r, respectively. As shown in Figure 2b, the subwavelength optical mode confinement in hybrid plasmonic waveguide results in an ultrasmall mode area down to 0.006 $(\lambda/2)^2$. The propagation length is calculated from $L_m = 1/[2\,\mathrm{Im}(\mathbf{k}_{eff})]$, where $\mathbf{k}_{eff}$ is the wavevector of the waveguide mode. As shown in Figure 2c, the hybrid plasmonic mode can travel through a long distance, which is more than 40 μm.

Figure 3a shows the electromagnetic field distributions of energy density W, electric field y component E_y, and electric field intensity $|E|^2$ for the hybrid plasmonic mode with TM polarization (where the electric field is perpendicular to the surface of the substrate) for different waveguide diameter d and air gap g. For large d and g (for example, $[d, g]$ = [500, 100]nm), the hybrid plasmonic waveguide supports a low-loss cylinder photonic-like

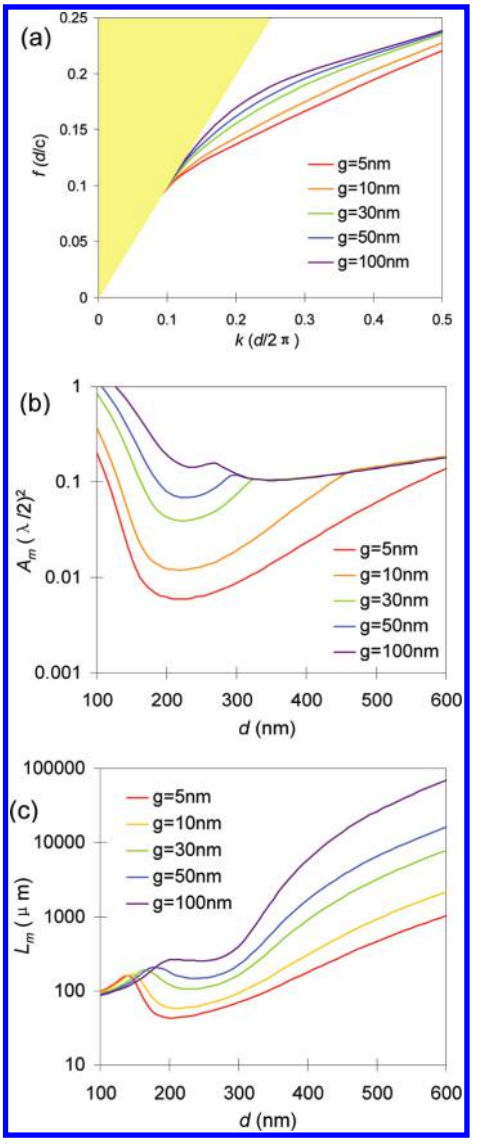

Figure 2. (a) The dispersion relation of the hybrid plasmonic mode with waveguide diameter d = 250 nm for different air gaps. (b) Mode area A_m of the hybrid plasmonic mode as functions of the waveguide diameter d and the air gap g. (c) The dependence of propagation length L_m on d and g for the hybrid plasmonic mode.

mode with optical energy confined in the dielectric waveguide core. For small d and g, the SPP-like mode will dominate with relatively high loss. For g in nanometer scale, for example $[d, g]$ = [250, 5]nm and $[d, g]$ = [500, 5]nm, the cylinder mode is strongly coupled to the SPP mode, and most of the optical energy is concentrated inside the air gap with ultrasmall mode area. For the dielectric substrate, as shown in Figure 3b, the optical energy is always confined inside the dielectric waveguide core to form a photonic mode, where the cylinder mode is evanescently coupled to the glass substrate.

With coupled mode theory, the eigenmode ψ supported in the coupled waveguide system can be described as the superposition of the cylinder mode ψ_{cyl} and the substrate mode ψ_{sub}

$$\psi = a\psi_{cyl} + b\psi_{sub} \quad (1)$$

where a and b are the mode amplitudes of the cylinder mode and the substrate mode with $b = (1 - |a|^2)^{1/2}$, and the coupled

dx.doi.org/10.1021/nl103070n |Nano Lett. 2011, 11, 321–328

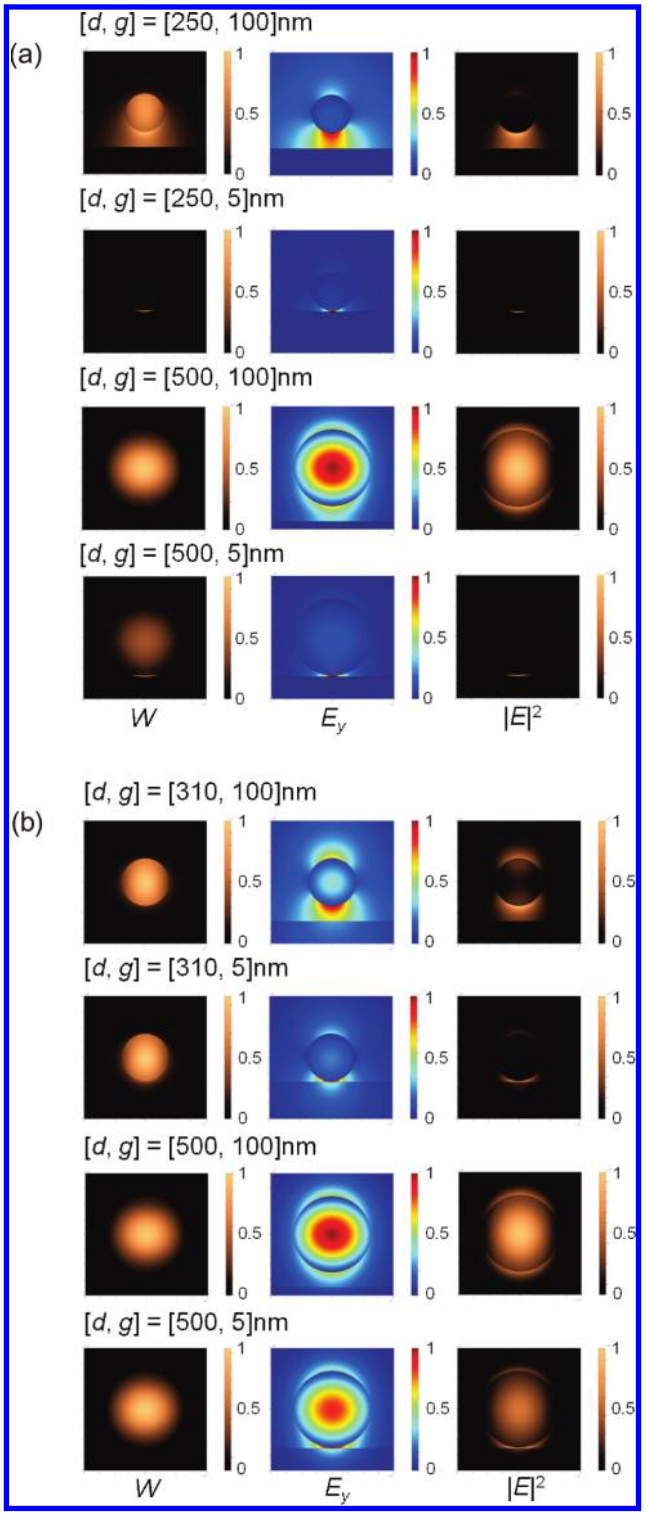

Figure 3. The distributions of electromagnetic energy density W, electric field y component E_y, and electric field intensity $|E|^2$ of (a) the hybrid plasmonic mode and (b) the photonic mode with different waveguide diameter d and air gap g.

waveguide system can be described as[26]

$$n_{cyl}a + \kappa b = n_{eff}a \quad (2)$$

$$\kappa a + n_{sub}b = n_{eff}b \quad (3)$$

where n_{sub} and n_{cyl} are the effective index of the substrate mode and the cylinder mode, n_{eff} is the effective index of the waveguide mode, and κ is the coupling strength between these two modes, which can be derived as

$$\kappa = \sqrt{(n_{eff} - n_{sub}) \cdot (n_{eff} - n_{cyl})} \quad (4)$$

Figure 4a,b plots the dependence of effective index n_{eff} on d and g for the hybrid plasmonic mode and the photonic mode, respectively. The glass substrate has refractive index of 1.45, which is much higher than the real part of the refractive index for the SPP mode in air−silver interface $n_{SPP} = (\varepsilon_m\varepsilon_d/(\varepsilon_m + \varepsilon_d))^{1/2} = 1.0039$. On the basis of eq 4, the effective index of the substrate mode n_{sub} limits the coupling strength κ between the cylinder waveguide mode and the substrate mode so that the coupling strength for the metallic substrate is much stronger than the dielectric substrate, as shown in Figure 4c,d. The coupling strength gets its maximum value when $n_{cyl} = n_{sub}$ at the critical diameter d_c of the cylinder waveguide, where the cylinder mode and substrate mode propagate in phase and the effective optical capacitance of the coupled system is maximized, so that the coupling between the two modes is strongest. The critical diameter d_c is ~300 nm for the hybrid plasmonic mode and ~340 nm for the photonic mode due to different substrate index. At the critical diameter with air gap $g = 5$ nm, κ_{max} is 0.93 for the hybrid plasmonic mode, while κ_{max} is only 0.22 for the photonic mode. The mode cutoff of the dielectric cylinder waveguide occurs when the diameter of the waveguide is less than 300 nm, so that the photonic mode suffers mode cutoff with optical leakage into the substrate and the coupling strength is dramatically reduced, as shown in Figure 4d. However, the hybrid plasmonic mode does not have mode cutoff so that the coupling is still very strong for d smaller than 300 nm, as shown in Figure 4c.

The coupling strength determines the optical energy concentration in the gap region, so as to the gradient optical force generated on the dielectric waveguide, which can be calculated by integrating the Maxwell's stress tensor (MST) $\mathbf{T}$ around any arbitrary surface enclosing the waveguide.[29] The time averaged optical force is

$$\langle \mathbf{F} \rangle = \int_S \langle \mathbf{T} \rangle \cdot \mathbf{n} da \quad (5)$$

where $\mathbf{T}$ is the Maxwell's stress tensor given by

$$\mathbf{T} = \varepsilon\varepsilon_0 \mathbf{EE} + \mu\mu_0 \mathbf{HH} - \frac{\mathbf{I}}{2}(\varepsilon\varepsilon_0 |\mathbf{E}|^2 + \mu\mu_0 |\mathbf{H}|^2) \quad (6)$$

S is a surface enclosing the cylinder waveguide, $\mathbf{n}$ is the unit normal vector to this surface, da is a differential element of surface area, and $\mathbf{I}$ is the identity tensor. Figure 4e,f shows the optical forces exerted on the dielectric waveguide without propagation loss, calculated from MST as the functions of d and g at unit input optical power for the hybrid plasmonic mode and the photonic mode, respectively. The maximum value of optical force for a fixed air gap occurs around $n_{cyl} = n_{sub}$, with d between 250 to 300 nm for the hybrid plasmonic mode and d around 310 nm for the photonic mode. For hybrid plasmonic mode with $d = 250$ nm, as the gap separation is reduced from 100 to 5 nm, the optical force increases from −5.6 to −149.2 pN μm^{-1} mW^{-1}. The negative value of optical force corresponds to attractive force applied on the dielectric waveguide. While for the photonic mode with $d = 310$ nm, as the gap separation is reduced

dx.doi.org/10.1021/nl103070n |Nano Lett. 2011, 11, 321–328

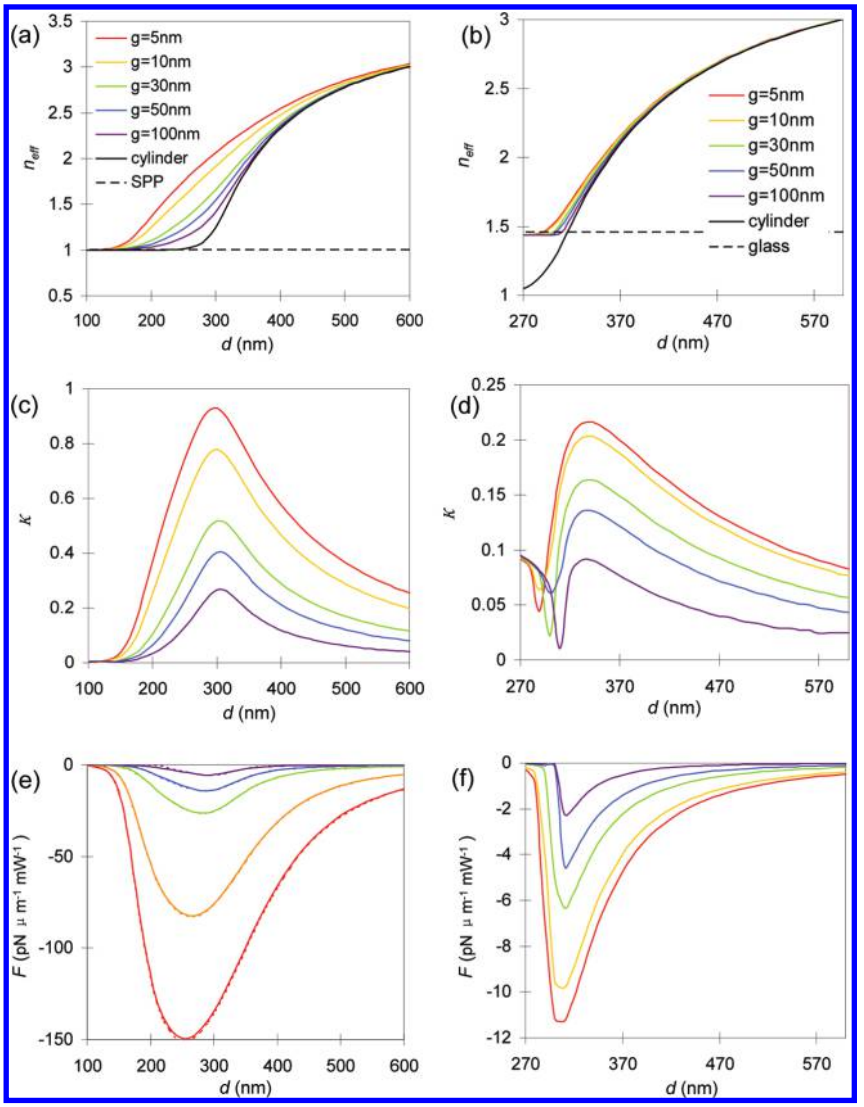

Figure 4. (a,b) The dependence of effective index n_{eff} on the waveguide diameter d and the air gap g for the hybrid plasmonic mode and the photonic mode, respectively. (c,d) The dependence of coupling strength κ on d and g for each kind of mode. (e,f) Optical attractive force exerted on the cylinder waveguide without propagation loss, calculated from MST as functions of d and g for the hybrid plasmonic mode and the photonic mode. The dashed lines in (e) are calculated from eq 7.

from 100 to 5 nm, the optical force only increases from −2.2 to −11.3 pN μm^{-1} mW^{-1}. The formation of the hybrid plasmonic mode gives rise to strong optical energy localization in the air gap so as to the enhanced gradient optical force, which is 1 order of magnitude larger than the optical force from the photonic mode. The optical force can also be obtained from the dispersion relation of the waveguide mode,[3,4]

$$F = -\left.\frac{\partial U}{\partial g}\right|_k = -\left.\frac{1}{\omega}\frac{\partial \omega}{\partial g}\right|_k U = \left.\frac{n_g}{n_{eff} c}\frac{\partial n_{eff}}{\partial g}\right|_k PL \qquad (7)$$

where the stored energy in the waveguide mode $U = n_g PL/c$ with the total optical power as P, the length of the waveguide is L, the group index is n_g, and the speed of light in vacuum is c. When the gap between the waveguide and the silver substrate is reduced, the eigenmode frequency ω of the hybrid plasmonic mode decreases for the same wavevector $\mathbf{k}$, indicating that an attractive optical force will be applied on the cylinder waveguide. The dashed lines in Figure 4e give the calculated optical forces based on eq 7, which match the MST results very well.

As the dielectric slot waveguide system has been widely studied for the optical forces enhancement,[3,5,8,14] here we also consider this type of waveguide system with two coupled silicon cylinder waveguides to compare with the hybrid plasmonic waveguide and the photonic waveguide. Figure 5a shows the electromagnetic field distributions of energy density W, electric field y component E_y, and electric field intensity $|E|^2$ for the slot waveguide mode with TM polarization (where the electric field is vertical) with waveguide diameter d = 300 nm. As the air gap decreases from 100 to 5 nm, the optical energy is concentrated inside the air gap region, and the mode area goes down to 0.012 $(\lambda/2)^2$ at g = 5 nm, which is slightly larger than the hybrid plasmonic mode with mode area of 0.009 $(\lambda/2)^2$ (as shown in Figure 2b). The deep subwavelength optical mode confinement in the slot waveguide mode will also enhance the optical forces. For comparison, Figure 5b plots the MST-calculated attractive optical forces exerted on the dielectric cylinder waveguide for the

dx.doi.org/10.1021/nl103070n |*Nano Lett.* 2011, 11, 321–328

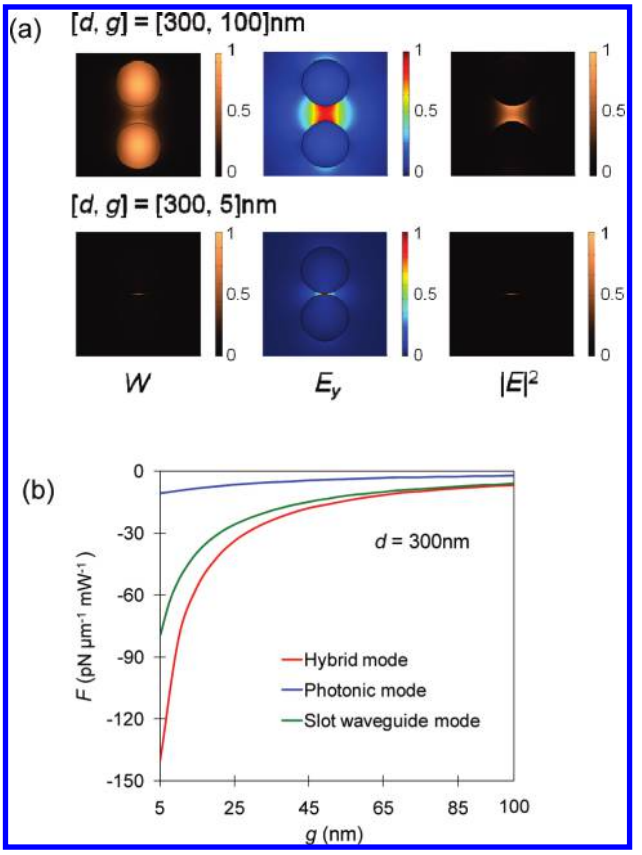

Figure 5. (a) The distributions of W, E_y, and $|E|^2$ of the slot waveguide mode with d = 300 nm and different air gap g. (b) The comparison of the optical forces applied on the dielectric cylinder waveguide for the hybrid mode, the photonic mode, and the slot waveguide mode with d = 300 nm and different air gap g.

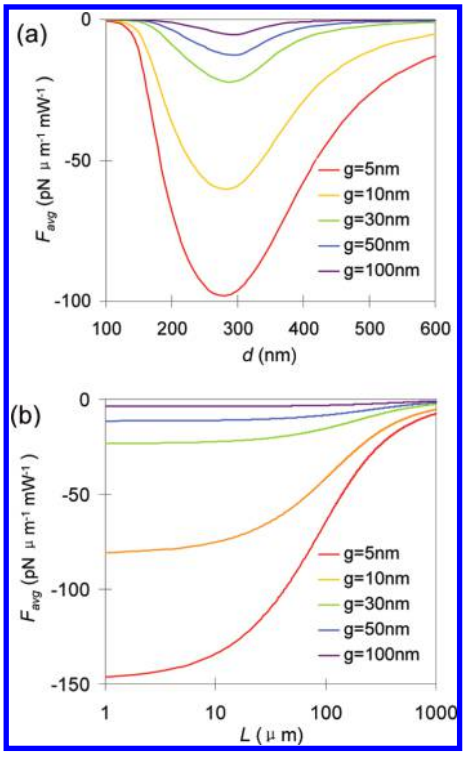

Figure 6. (a) The averaged optical force with propagation loss F_{avg} along the waveguide with length L = 50 μm for the hybrid plasmonic mode. (b) The dependence of F_{avg} on waveguide length L with various air gaps for the hybrid plasmonic mode.

hybrid mode, the photonic mode and the slot waveguide mode, with d = 300 nm and different air gap g. It is clear that the optical force generated from the hybrid mode is stronger than the force from the slot waveguide mode. For example, at g = 5 nm, the optical force is −140 pN μm^{-1} mW^{-1} for the hybrid mode, while it is −80 pN μm^{-1} mW^{-1} for the slot waveguide mode.

For hybrid plasmonic mode, the optical force per unit length $F(z)$ at position z depends on the total optical power of the waveguide mode $P(z)$, which will exponentially decay along the waveguide with propagation length L_m due to the ohmic loss. The averaged optical force per unit length with propagation loss along the waveguide with length L can be calculated as

$$F_{avg} = \frac{F_0}{L}\int_0^L \exp\left(\frac{-z}{L_m}\right)dz \qquad (8)$$

where F_0 is the optical force without propagation loss. For waveguide with length L = 50 μm, the averaged optical force F_{avg} for the hybrid plasmonic mode given in Figure 6a is still much higher than the optical force from the photonic mode shown in Figure 4f. For example, with d = 280 nm, as the gap separation is reduced from 100 to 5 nm, the optical force increases from −5.2 to −98.1 pN μm^{-1} mW^{-1}. Figure 6b shows the averaged optical forces as functions of waveguide length L with d = 250 nm for the hybrid plasmonic mode, which shows that the optical force mediated from the hybrid plasmonic mode is much stronger than that created from the photonic mode for a broad range of waveguide length, even with the propagation loss considered. This implies that practical demonstrations and applications are feasible.

The greatly enhanced optical energy concentration as well as the field gradient in the gap region also allows efficient trapping of single nanoscale particle. Optical trapping have been widely used for capturing and handling of dielectric objects with micrometer size in various applications such as single cell manipulation and flow cytometry. However, optical diffraction significantly limits the trapping strength and the minimum size of the trapped particles in traditional optical tweezers. Nanoscale optical traps with near-field approaches can focus light tightly into subwavelength volume to enhance the optical trapping forces, so that dielectric nanoparticles with size down to 50 nm can be trapped and manipulated precisely.[22−25] Here we show a new type of nanoscale optical traps based on extremely strong optical field gradients within hybrid plasmonic waveguides, enabling trapping of single nanoparticle with diameter of only several nanometers at low input optical power.

Optical trapping force is proportional to the gradient of the electrical field distribution[22]

$$F = -\nabla U = -\nabla(PE) = -\frac{n_m}{2}\alpha\nabla E^2 \qquad (9)$$

where U is the optical trapping potential, P is the induced nanoparticle dipole moment, α is the polarizability of the nanoparticle, and n_m is the refractive index of the medium surrounding the particle. For a single beam gradient optical force trap, the gradient force applied on a Rayleigh particle (with diameter 2r much

dx.doi.org/10.1021/nl103070n |Nano Lett. 2011, 11, 321–328

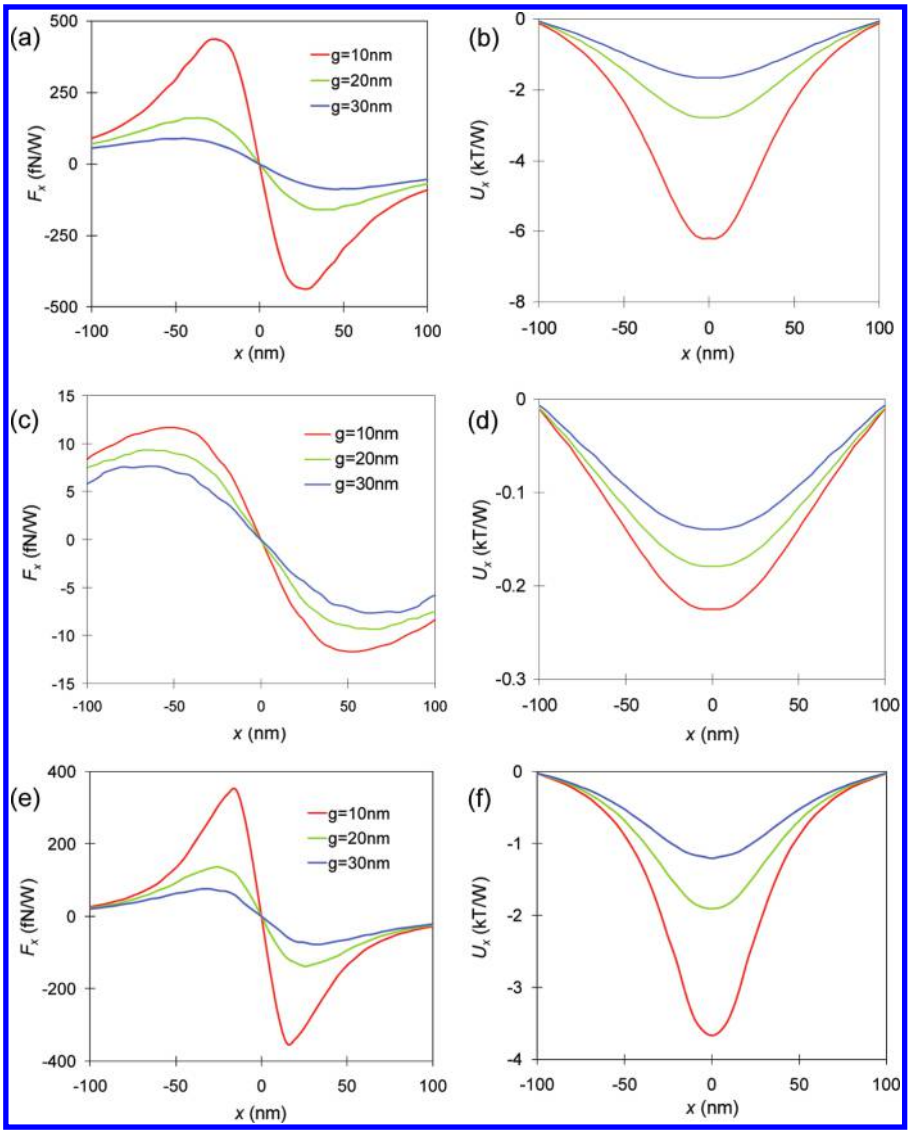

Figure 7. (a,c,e) Optical trapping forces along x direction F_x applied on a single polystyrene nanoparticle of 5 nm diameter for the hybrid plasmonic mode, the photonic mode, and the slot waveguide mode with d = 220 nm and gaps of 10, 20, and 30 nm. (b,d,f) Optical trapping potential along x direction U_x for the hybrid plasmonic mode, the photonic mode, and the slot waveguide mode.

less than the wavelength λ) is given by[30]

$$F = -\frac{n_m^3 r^3}{2}\left(\frac{m^2-1}{m^2-2}\right)\nabla E^2 \qquad (10)$$

where m is the ratio of the refractive indices of particle and environmental medium. The optical trapping force is proportional to r^3 so that it will be extremely difficult to trap nanoparticles with diameter less than 14 nm with 1.5 W optical power of the trapping beam, as demonstrated experimentally.[30]

The hybridization between the surface plasmon mode and waveguide mode creates strong optical confinement in the gap region, which will enhance the optical trapping force and enable to trap single dielectric nanoparticle. Figure 1b illustrates the geometry of the coupled waveguide system for the optical trapping of a single nanoparticle. The diameter of the waveguide is 220 nm. A polystyrene nanoparticle with refractive index n = 1.59 with diameter of 5 nm is used for studying the optical trapping effects. The medium around the waveguide is water with refractive index of n_m = 1.33. The three-dimensional simulations are performed in COMSOL, and the gradient forces for a nanoparticle at different positions along the x axis (from −100 to 100 nm) are calculated with the Maxwell's stress tensor (MST) over the surface enclosing the nanoparticle. Note that the perturbation to the hybrid plasmonic mode due to the existence of the nanoparticle in the gap region is pretty weak, since the size of the nanoparticle is much smaller than the wavelength, and it also has a low refractive index compared to the silicon waveguide.

Figure 7a,c,e shows the optical trapping force along x direction F_x applied on a single nanoparticle with diameter of 5 nm for the hybrid plasmonic mode, the photonic mode, and the slot waveguide mode, respectively. The maximum optical trapping force occurs at the position where the optical field gradient is largest, as indicated in eq 9. As the gap separation reduces, the optical trapping force increases. At g = 10 nm, the maximum optical trapping force at unit input optical power is 435 fN/W for the hybrid plasmonic mode, and it is 350 fN/W for the slot waveguide mode. However, the trapping force is only 11.6 fN/W

dx.doi.org/10.1021/nl103070n |*Nano Lett.* 2011, 11, 321–328

for the photonic mode. The sign of the trapping force is flipped when the particle moves across the $x = 0$ point, indicating that the particle can be trapped right underneath the waveguide. The optical trapping potential profiles along x direction with trapping force integration are shown in Figure 7b,d,f for the three systems, respectively. The zero point of the potential is defined as the particle is 100 nm away from the waveguide center ($x = -100$ nm). Right underneath the waveguide, the optical trapping potential U_x is around 6.2 k_BT/W for the hybrid mode at $g = 10$ nm, where the Boltzmann term k_BT is used to represent the random thermal energy of the nanoparticle due to Brownian motion. And U_x is around 3.6 k_BT/W for the slot waveguide mode at $g = 10$ nm. Since U_x around $x = 0$ is much larger than the Brownian motion k_BT, the stable trapping of a single particle can be realized for both the hybrid mode and the slot waveguide mode. The trapping region with $|U| > k_BT$ is around 150 nm along x direction for the hybrid mode, and it is around 100 nm for the slot waveguide mode, which are much less than the wavelength. For the photonic mode, the maximum trapping potential at $x = 0$ is only around 0.22 k_BT/W so that there is no optical trapping effect for the nanoparticle. The enhancement of the optical trapping potential for the nanoparticle from the hybrid plasmonic mode is approximately 30 times stronger than the one in the photonic mode due to its strong localization of the optical field in the gap region. The ability to transport the nanoparticle along the waveguide propagation direction is also studied by calculating the optical propulsion forces along the waveguide F_z applied on the nanoparticle. The results show that F_z in the hybrid plasmonic mode is more than 1 order of magnitude stronger than the force in the photonic mode. For example, with $g = 10$ nm, F_z is 45 fN/W for the hybrid mode at $x = 0$, while the photonic mode only has 3.5 fN/W. This is due to the strong optical scattering on the nanoparticle from the highly focused hybrid plasmonic mode. The optical trapping force and propulsion force can be significantly enhanced furthermore with high-Q hybrid plasmonic resonators[31] as the total optical energy is amplified due to the long photon lifetime in the resonator.

In conclusion, we have demonstrated that the optical force exerted on the dielectric waveguide in the hybrid plasmonic waveguide is more than 1 order of magnitude stronger than the optical force created in the photonic waveguide with dielectric substrate, which is due to the strong coupling between the cylinder waveguide mode and the surface plasmon mode supported by the substrate. The mechanism of this enhanced optical force is analyzed based on both Maxwell's stress tensor formalism and the coupled mode theory. In addition, we have demonstrated that the optical trapping force applied on a single dielectric nanoscale particle in the hybrid plasmonic waveguide is much stronger than that in the photonic waveguide. The strongly enhanced optical trapping force enables the applications of optical tweezers at nanometer scale, opening a new realm of the optical trapping and manipulation of single nanoparticles such as biomolecules and quantum dots for many exciting applications.

AUTHOR INFORMATION

Corresponding Author
*E-mail: xiang@berkeley.edu.

ACKNOWLEDGMENT

This work was supported by the U.S. Department of Energy under Contract No. DE-AC02-05CH11231.

REFERENCES

(1) Ashkin, A. Acceleration and trapping of particles by radiation pressure. *Phys. Rev. Lett.* **1970**, *24*, 156.
(2) Chu, S. Laser manipulation of atoms and particles. *Science* **1991**, *253*, 861–866.
(3) Povinelli, M. L.; et al. Evanescent-wave bonding between optical waveguides. *Opt. Lett.* **2005**, *30*, 3042–3044.
(4) Li, M.; et al. Harnessing optical forces in integrated photonic circuits. *Nature* **2008**, *456*, 480.
(5) Li, M.; Pernice, W. H. P.; Tang, H. X. Tunable bipolar optical interactions between guided lightwaves. *Nat. Photonics* **2009**, *3*, 464.
(6) Povinelli, M. L.; et al. High-Q enhancement of attractive and repulsive optical forces between coupled whispering-gallery-mode resonators. *Opt. Express* **2005**, *13*, 8286.
(7) Rakich, P.; Popović, M. A.; Soljačić, M.; Ippen, E. P. Trapping, corralling and spectral bonding of optical resonances through optically induced potentials. *Nat. Photonics* **2007**, *1*, 658.
(8) Eichenfield, M.; Camacho, R.; Chan, J.; Vahala, K. J.; Painter, O. A picogram- and nanometre-scale photonic-crystal optomechanical cavity. *Nature* **2009**, *459*, 550.
(9) Wiederhecker, G. S.; Chen, L.; Gondarenko, A.; Lipson, M. Controlling photonic structures using optical forces. *Nature* **2009**, *462*, 633.
(10) Kippenberg, T. J.; Vahala, K. J. Cavity Optomechanics: Back-Action at the Mesoscale. *Science* **2008**, *321*, 1172.
(11) Notomi, M.; Taniyama, H.; Mitsugi, S.; Kuramochi, E. Optomechanical wavelength and energy conversion in high-Q double-layer cavities of photonic crystal slabs. *Phys. Rev. Lett.* **2006**, *97*, No. 023903.
(12) Rosenberg, J.; Lin, Q.; Painter, O. Static and dynamic wavelength routing via the gradient optical force. *Nat. Photonics* **2009**, *3*, 478.
(13) Anetsberger, G.; et al. Near-field cavity optomechanics with nanomechanical oscillators. *Nat. Phys.* **2009**, *5*, 909.
(14) Yang, A. H. J.; et al. Optical manipulation of nanoparticles and biomolecules in sub-wavelength slot waveguides. *Nature* **2009**, *457*, 71.
(15) Mandal, S.; Serey, X.; Erickson, D. Nanomanipulation Using Silicon Photonic Crystal Resonators. *Nano Lett.* **2010**, *10*, 99.
(16) Barnes, W. L.; Dereux, A.; Ebbesen, T. W. Surface plasmon subwavelength optics. *Nature* **2003**, *424*, 824–830.
(17) Schuller, J. A.; Barnard, E. S.; Cai, W.; Jun, Y. C.; White, J. S.; Brongersma, M. L. Plasmonics for extreme light concentration and manipulation. *Nat. Mater.* **2010**, *9*, 193.
(18) Ishikawa, A.; Zhang, S.; Genov, D. A.; Bartal, G.; Zhang, X. Deep subwavelength terahertz waveguides using gap magnetic plasmon. *Phys. Rev. Lett.* **2009**, *102*, 043904.
(19) Choi, H.; Pile, D. F.; Nam, S.; Bartal, G.; Zhang, X. Compressing surface plasmons for nano-scale optical focusing. *Opt. Express* **2009**, *17*, 7519.
(20) Nome, R. A.; Guffey, M. J.; Scherer, N. F.; Gray, S. K. Plasmonic Interactions and Optical Forces between Au Bipyramidal Nanoparticle Dimers. *J. Phys. Chem. A* **2009**, *113*, 4408.
(21) Woolf, D.; Loncar, M.; Capasso, F. The forces from coupled surface plasmon polaritons in planar waveguides. *Opt. Express* **2009**, *17*, 19996.
(22) Xu, H.; Käll, M. Surface-Plasmon-Enhanced Optical Forces in Silver Nanoaggregates. *Phys. Rev. Lett.* **2002**, *89*, No. 246802.
(23) Grigorenko, A. N.; Roberts, N. W.; Dickinson, M. R.; Zhang, Y. Nanometric optical tweezers based on nanostructured substrates. *Nat. Photonics* **2008**, *2*, 365.
(24) Righini, M.; Zelenina, A. S.; Girard, C.; Quidant, R. Parallel and selective trapping in a patterned plasmonic landscape. *Nat. Phys.* **2007**, *3*, 477.
(25) Juan, M. L.; Gordon, R.; Pang, Y.; Eftekhari, F.; Quidant, R. Self-induced back-action optical trapping of dielectric nanoparticles. *Nat. Phys.* **2009**, *5*, 915.
(26) Oulton, R. F.; Sorger, V.; Genov, D. A.; Pile, D. F. P.; Zhang, X. A hybrid plasmonic waveguide for subwavelength confinement and long-range propagation. *Nat. Photonics* **2008**, *2*, 496.

(27) Oulton, R. F.; et al. Plasmon lasers at deep subwavelength scale. *Nature* **2009**, *461*, 629–632.
(28) Johnson, P. B.; Christie, R. W. Optical constants of the noble metals. *Phys. Rev. B* **1972**, *6*, 4370.
(29) Jackson, J. D., *Classical Electrodynamics*; Hamilton Printing Co.: Castleton, NY, 1998.
(30) Ashkin, A.; Dziedzic, J. M.; Bjorkholm, J. E.; Chu, S. Observation of a single-beam gradient force optical trap for dielectric particles. *Opt. Lett.* **1986**, *11*, 288.
(31) Xiao, Y.; et al. High quality factor, small mode volume, ring-type plasmonic microresonator on a silver chip. *J. Phys. B: At. Mol. Opt. Phys.* **2010**, *43*, No. 035402.

■ NOTE ADDED AFTER ASAP PUBLICATION

This paper published ASAP January 13, 2011 with an incomplete reference list. References 18 and 19 were added to the reference list in the version published January 18, 2011.